

N-Acetyltransferase 2 Genotype-Dependent N-Acetylation of Hydralazine in Human Hepatocytes

Cecily E. Allen, Mark A. Doll, and David W. Hein

Department of Pharmacology and Toxicology and James Graham Brown Cancer Center, University of Louisville School of Medicine, Louisville, Kentucky

Received September 8, 2017; accepted October 6, 2017

ABSTRACT

Hydralazine is used in the treatment of essential hypertension and is under investigation for epigenetic therapy in the treatment of neoplastic and renal diseases. N-acetyltransferase (NAT) 2 exhibits a common genetic polymorphism in human populations. After recombinant expression in yeast, human NAT2 exhibited an apparent Lineweaver-Burk constant (K_m) value ($20.1 \pm 8.8 \mu\text{M}$) for hydralazine over 20-fold lower than the apparent K_m value ($456 \pm 57 \mu\text{M}$) for recombinant human NAT1 ($P = 0.0016$). The apparent V_{max} value for recombinant human NAT1 ($72.2 \pm 17.9 \text{ nmol acetylated/min/mg protein}$) was significantly ($P = 0.0245$) lower than recombinant human NAT2 ($153 \pm 15 \text{ nmol acetylated/min/mg protein}$), reflecting 50-fold higher clearance for recombinant human NAT2. Hydralazine NAT activities exhibited a robust acetylator gene dose response in cryopreserved

human hepatocytes both in vitro and in situ. Hydralazine NAT activities in vitro differed significantly with respect to NAT2 genotype at 1000 ($P = 0.0319$), 100 ($P = 0.002$), and 10 μM hydralazine ($P = 0.0029$). Hydralazine NAT activities differed significantly ($P < 0.001$) among slow acetylator hepatocytes, ($\text{NAT2}^*5\text{B}/^*5\text{B} > \text{NAT2}^*5\text{B}/^*6\text{A} > \text{NAT2}^*6\text{A}/^*6\text{A}$). The in situ hydralazine N-acetylation rates differed significantly with respect to NAT2 genotype after incubation with 10 ($P = 0.002$) or 100 μM ($P = 0.0015$) hydralazine and were higher after incubation with 100 μM (10-fold) than with 10 μM (4.5-fold) hydralazine. Our results clearly document NAT2 genotype-dependent N-acetylation of hydralazine in human hepatocytes, suggesting that hydralazine efficacy and safety could be improved by NAT2 genotype-dependent dosing strategies.

Introduction

Hydralazine has been used for decades in the treatment of hypertension and is indicated in the long-term therapy of essential hypertension, in the short-term therapy of pregnancy-induced hypertension and eclampsia, and in the therapy of hypertensive crisis (Cohn et al., 2011). Hydralazine is one of the first line antihypertensive agents used to treat severe hypertension in pregnancy (Magee et al., 2003). More recently, hydralazine also has been shown to attenuate the progression of chronic kidney disease (Tampe et al., 2015).

Hydralazine is currently in clinical trials in combination with valproate for epigenetic cancer therapy (reviewed in Dueñas-Gonzalez et al., 2014). Methylation at CpG regions in DNA promoters is a common alteration of neoplastic cells leading to uncontrolled proliferation via suppression of tumor suppressor genes. Hydralazine is a non-nucleoside inhibitor of DNA methylation (Chuang et al., 2005; Segura-Pacheco et al., 2006; Singh et al., 2009, 2013; Castillo-Aguilera et al., 2017). Studies have demonstrated the ability of hydralazine to increase sensitivity to chemotherapeutic agents, to decrease the expression of cell cycle genes, and to increase DNA damage, resulting in growth inhibition mediated through epidermal growth factor signaling pathways (Coronel et al., 2011; Graca et al., 2014; Castillo-Aguilera et al., 2017).

This study was partially supported by US Public Health Service National Institutes of Health Grants [R25-CA134283 and P20-GM113226].
<https://doi.org/10.1124/dmd.117.078543>.

Arylamine N-acetyltransferase (NAT) 1 and NAT2 catalyze the N-acetylation of hydralazine and numerous arylamine drugs/xenobiotic agents (reviewed in Hein, 2009). Because NAT2 is expressed mainly in the liver and gastrointestinal tract, it is often involved in drug metabolism (McDonagh et al., 2014). NAT2 expresses common genetic polymorphisms in human populations, resulting in rapid, intermediate, and slow acetylator phenotypes (Hein, 2009). Previous studies (Shepherd et al., 1981) showed 15-fold differences in hydralazine plasma concentrations between rapid and slow acetylators of the probe drug sulfamethazine after administration of the same dose of hydralazine. Since acetylator phenotype has been shown to modify plasma levels of hydralazine, acetylator phenotype- or genotype-dependent dosing strategies have been both suggested and implemented (described further in the *Discussion*).

N-acetylation of hydralazine generates an unstable N-acetylated intermediate that spontaneously converts to 3-methyl-s-triazolo [3,4a]-phthalazine (MTP) (reviewed in Weber and Hein, 1985). Although the differential plasma levels of hydralazine in rapid and slow acetylators strongly implicate an important role for NAT2 in hydralazine metabolism, the possible role of NAT1 and the comparative affinity of hydralazine for N-acetylation via NAT1 or NAT2 has not been reported.

The purposes of the present study were 1) to assess the relative ability and affinity of human NAT1 or NAT2 to catalyze the N-acetylation of hydralazine and 2) to investigate the role of NAT2 genotype on N-acetylation rates both in vitro and in situ in cryopreserved human hepatocytes. The results are important for the refinement of hydralazine dosing strategies, particularly in clinical trials investigating its possible efficacy as an epigenetic drug in the treatment of neoplastic and renal diseases.

ABBREVIATIONS: HPLC, high-performance liquid chromatography; K_m , Lineweaver-Burk constant; MTP, 3-methyl-s-triazolo [3,4a]-phthalazine; NAT, N-acetyltransferase; PBS, phosphate-buffered saline.

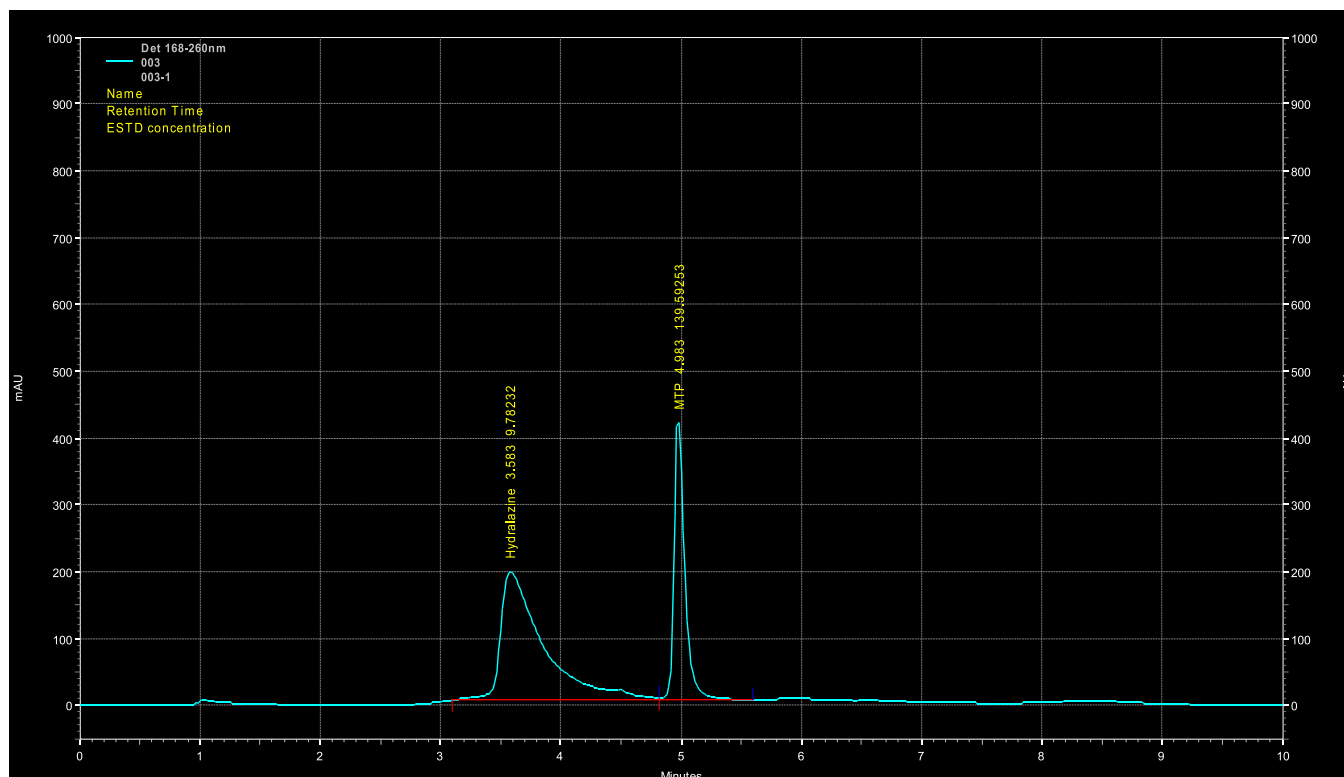


Fig. 1. HPLC separation of hydralazine and MTP. AU, absorbance units.

Materials and Methods

Production of Recombinant Human *N*-Acetyltransferases. The coding regions of *NAT1*4* (reference *NAT1*) and *NAT2*4* (reference *NAT2*) were amplified by polymerase chain reaction using previously constructed plasmids, as previously described (Hein and Doll, 2017). The yeast vector pESP-3 (Stratagene, La Jolla, CA) was digested with *NdeI* and *AscI* at 37°C overnight and gel purified. Purified polymerase chain reaction products and 80 ng of plasmid were ligated overnight at 16°C with T4 DNA ligase (New England BioLabs Inc., Beverly, MA). Ligated plasmids were transformed into XL-10 Gold Ultracompetent *Escherichia coli* (Stratagene). Plasmids were isolated from cultures grown from selected colonies using the Plasmid Midi Kit (QIAGEN, Valencia, CA) and sequenced using ThermoSequenase (Amersham, Arlington Heights, IL). Constructs were then transformed into competent *Schizosaccharomyces pombe* and expressed following the manufacturer instructions (Stratagene). Mock-transformed yeast used pESP-3 vector with no *NAT2* insert. Total cell lysates were prepared by vigorous agitation of yeast in ice-cold 20 mM NaPO₄, 1 mM dithiothreitol, 1 mM EDTA, 0.2% Triton X-100, 1 mM phenylmethylsulfonyl fluoride, 1 μM pepstatin A, and 1 μg/ml aprotinin containing acid-washed glass beads (Stratagene) for 10 minutes at 4°C. Liquid fractions were collected from the lysed cells and centrifuged at 13,000g for 20 minutes. Supernatants were collected, aliquoted, and stored at -70°C until used for enzymatic assays. To mitigate possible instability of human *NAT1* and *NAT2*, supernatant aliquots were thawed only once and used immediately to carry out the enzymatic reactions. Apparent V_{max} and apparent Lineweaver-Burk constant (K_m) values were determined by nonlinear regression of the Michaelis-Menten equation (GraphPad Software, San Diego, CA). Protein concentrations were determined using the BIO-RAD (Richmond, CA) Protein Assay Kit.

Source and Processing of Cryopreserved Human Hepatocytes. Cryopreserved human hepatocytes were received from BioreclamationIVT (Baltimore, MD) and stored in liquid nitrogen until use. Upon removal from liquid nitrogen, hepatocytes were thawed according to the manufacturer instructions by warming a vial of the hepatocytes at 37°C for 90 seconds and transferring them to a 50 ml conical tube containing 45 ml of InVitroGRO HT medium (BioreclamationIVT). The suspension was centrifuged at 50g at room temperature for 5 minutes. The supernatant was discarded, and cells were washed once in ice-cold

phosphate-buffered saline (PBS) before lysing the cells in ice-cold 20 mM NaPO₄, 1 mM dithiothreitol, 1 mM EDTA, 0.2% Triton X-100, 1 mM phenylmethylsulfonyl fluoride, 1 μM pepstatin A, and 1 μg/ml aprotinin. The lysate was centrifuged at 15,000g for 20 minutes, and the supernatant was aliquoted and stored at -70°C. To mitigate the possible instability of human *NAT1* and *NAT2*, supernatant aliquots were thawed only once and used immediately to carry out the enzymatic reactions.

Determination of *NAT2* Genotype and Deduced Phenotype. Genomic DNA was isolated from pelleted cells prepared from human cryopreserved hepatocyte samples as described above using the QIAamp DNA Mini Kit (QIAGEN) according to the manufacturer instructions. *NAT2* genotypes and deduced phenotypes were determined as described previously (Doll and Hein, 2001). Controls (no DNA template) were run to ensure that there was no amplification of contaminating DNA.

Measurement of Hydralazine *N*-Acetyltransferase Activity In Vitro. *NAT* assays containing yeast or hepatocyte lysate (<2 mg protein/ml), 10–1000 μM hydralazine, and 1 mM acetyl CoA were incubated at 37°C. Reactions were terminated by the addition of 1:10 volume of 1 M acetic acid, and the reaction tubes were centrifuged in a small biofuge at 15,000g for 10 minutes to precipitate protein. The amount of acetyl-hydralazine produced (measured as MTP) was determined after separation and quantitation by high-performance liquid chromatography (HPLC). Separation of hydralazine and MTP was accomplished by injection (40 μl) onto a 125 × 4 mm Lichrospher 100 RP-100 5 μM C18 HPLC column subjected to a gradient of 100% 20 mM sodium perchlorate pH 2.5/0% acetonitrile to 50% 20 mM sodium perchlorate pH 2.5/50% acetonitrile over 5 minutes. Hydralazine and MTP were eluted at 3.58 and 4.98 minutes, respectively (Fig. 1). The intra-assay HPLC coefficient of variation was 2.56% for hydralazine and 1.66% for MTP with an MTP limit of detection of 100 pmol/40 μl. Protein concentrations were determined using the BIO-RAD Protein Assay Kit.

Cryopreserved human hepatocytes were selected at random with rapid genotypes *NAT2*4/*4* [$n = 6$; (three males and three females)]; intermediate genotypes *NAT2*4/*5B* ($n = 3$) and *NAT2*4/*6A* ($n = 2$) (three males and two females); and slow genotypes *NAT2*6A/*6A* ($n = 2$), *NAT2*6A/*7B* ($n = 1$), *NAT2*5B/*5B* ($n = 1$), and *NAT2*5B/*6A* ($n = 1$) (four males and one sex

unknown]. To further explore genetic heterogeneity in the slow acetylator genotype, additional assays were conducted with 300 μM hydralazine and 1 mM acetyl CoA in cryopreserved human hepatocytes with genotypes $\text{NAT2}^*5/^*5$ ($n = 5$; three males and two females), $\text{NAT2}^*5/^*6$ ($n = 6$; 3 males and 3 females), and $\text{NAT2}^*6/^*6$ ($n = 5$; three males and two females).

Measurement of Hydralazine *N*-Acetylation In Situ. Cryopreserved human hepatocytes previously identified as rapid, intermediate, or slow NAT2 acetylator genotypes (Doll et al., 2017) were thawed as described above and transferred to 50 ml conical tubes containing 12 ml of InVivoGRO CP media. One milliliter of hepatocyte/media mixture was transferred to each well of 12-well BioCoat (Corning, Corning, NY) collagen-coated plates to allow cells to attach for 48 hours at 37°C. After culture in growth media for 48 hours, the cells were washed three times with 500 μl 1 \times PBS and replaced with PBS + dextrose and hydralazine concentrations from 0 to 100 μM . Hepatocytes were incubated for up to 12 hours, after which media were removed and protein was precipitated by the addition of a 1:10 volume of 1 M acetic acid. Media were centrifuged at 15,000g for 10 minutes, and supernatant was used to separate and quantitate hydralazine and MTP by HPLC as described above. The cell number was determined after 12 hours of incubation with hydralazine, and activity was calculated in nanomoles of acetylated product per 12 hours per million cells in rapid genotypes $\text{NAT2}^*4/^*4$ ($n = 5$) (two males and three females); intermediate genotypes $\text{NAT2}^*4/^*5\text{B}$ ($n = 4$) and $\text{NAT2}^*4/^*6\text{A}$ ($n = 1$) (two males, one female, and two with sex unknown); and slow genotypes $\text{NAT2}^*5\text{B}/^*6\text{A}$ ($n = 2$), $\text{NAT2}^*5\text{B}/^*5\text{B}$ ($n = 2$), and $\text{NAT2}^*6\text{A}/^*6\text{A}$ ($n = 1$) (four males and one with sex unknown).

Statistical Analysis. Differences in *N*-acetylation rates among rapid, intermediate, and slow NAT2 acetylator genotypes were tested for significance by one-way analysis of variance followed by Tukey-Kramer multiple-comparisons test (GraphPad Software).

Results

Michaelis-Menten Kinetic Constants for Hydralazine *N*-Acetylation Catalyzed by Recombinant Human NAT1 and NAT2.

Apparent K_m and V_{max} values were calculated for human recombinant NAT1 and NAT2 (Fig. 2). After recombinant expression in yeast, human NAT2 exhibited an apparent K_m value ($20.1 \pm 8.8 \mu\text{M}$) over 20-fold lower than the apparent K_m value ($456 \pm 57 \mu\text{M}$) for recombinant human NAT1 ($P = 0.0016$). The apparent V_{max} for recombinant human NAT1 ($72.2 \pm 17.9 \text{ nmol acetylated/min/mg protein}$) was significantly ($P = 0.0245$) lower than for recombinant human NAT2 ($153 \pm 15 \text{ nmol acetylated/min/mg protein}$), which reflects a 50-fold higher clearance for recombinant human NAT2 than for NAT1.

Hydralazine *N*-Acetyltransferase Activity In Vitro from Cryopreserved Human Hepatocytes. Hydralazine NAT activities exhibited a robust and significant acetylator gene dose-response in vitro from human cryopreserved human hepatocytes. At concentrations of hydralazine ranging from 10 to 1000 μM , the hydralazine NAT activities differed significantly between NAT2 acetylator phenotypes at 1000 ($P = 0.0319$), 100 ($P = 0.002$), and 10 μM hydralazine ($P = 0.0029$). The highest levels were observed in rapid acetylator, lower levels in intermediate acetylator, and the lowest levels in slow acetylator hepatocytes (Fig. 3). Mean hydralazine NAT activities in the intermediate acetylators were very similar to the arithmetic average between the rapid and slow acetylators at each hydralazine concentration.

Genetic heterogeneity was observed among slow acetylator genotypes. Hydralazine NAT activities differed significantly ($P < 0.001$) among the slow acetylator hepatocytes. Highest levels in $\text{NAT2}^*5\text{B}/^*5\text{B}$, lower levels in $\text{NAT2}^*5\text{B}/^*6\text{A}$, and the lowest levels in $\text{NAT2}^*6\text{A}/^*6\text{A}$ hepatocytes (Fig. 4).

Hydralazine *N*-Acetylation In Situ in Cryopreserved Human Hepatocytes. Hydralazine was unstable in various culture media but stable in PBS as measured by HPLC. Therefore, after plating hepatocytes in the normal growth media for 48 hours, hepatocytes were washed with PBS and incubated with PBS + dextrose when adding hydralazine.

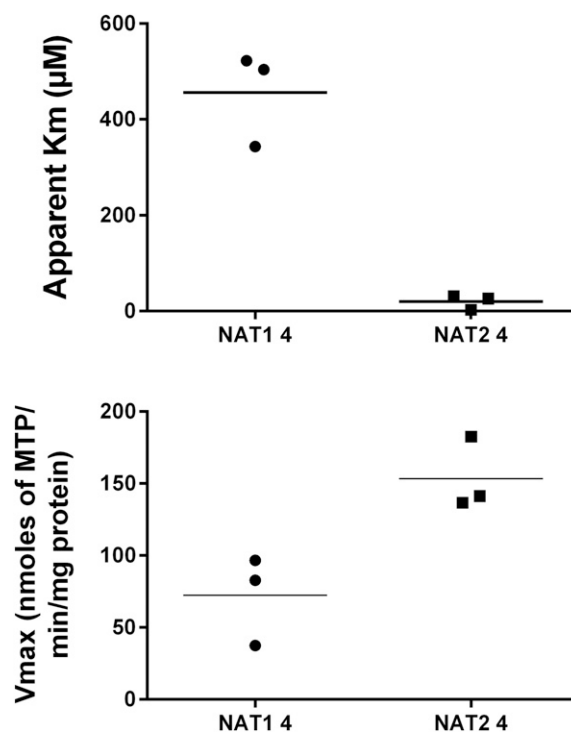


Fig. 2. Recombinant human NAT1 and NAT2 Michaelis-Menten kinetic constants for hydralazine. Scatter plots illustrate data from three independent measurements with the mean shown by the horizontal line. The apparent K_m value for hydralazine was significantly ($P = 0.0016$) higher for recombinant human NAT1 ($456 \pm 57 \mu\text{M}$) than for NAT2 ($20.1 \pm 8.8 \mu\text{M}$). The apparent V_{max} value for hydralazine *N*-acetylation was significantly ($P = 0.0245$) lower for recombinant NAT1 ($72.2 \pm 17.9 \text{ nmol acetylated/min/mg protein}$) than NAT2 ($153 \pm 15 \text{ nmol acetylated/min/mg protein}$).

Under these conditions, in situ hydralazine *N*-acetylation in cryopreserved human hepatocytes was both concentration and time dependent (Fig. 5). Hydralazine *N*-acetylation rates differed significantly among rapid, intermediate, and slow acetylator hepatocytes after incubation with 10 ($P = 0.002$) or 100 μM ($P = 0.0015$) hydralazine with the highest levels in rapid acetylator, lower levels in intermediate acetylator, and the lowest levels in slow acetylator cryopreserved human hepatocytes (Fig. 6). Differences in the mean values for hydralazine *N*-acetylation rates between homozygous rapid and slow acetylators were higher after incubation with 100 μM (10-fold) than 10 μM (4.5-fold) hydralazine.

Discussion

As recently reviewed (McDonagh et al., 2014), hydralazine treatment of hypertension and resistant hypertension is affected by acetylator phenotype. In early studies (Shepherd et al., 1981) in patients with hypertension, hydralazine plasma concentrations varied as much as 15-fold among individuals reflecting an “acetylator index” in the *N*-acetylation of the probe drug (sulfamethazine) used to determine acetylator phenotype.

More recently, hydralazine plasma levels were evaluated in 26 healthy volunteers (13 slow, 0 intermediate, and 13 rapid acetylators) after a single oral dose of 182 mg of a controlled-release hydralazine tablet (Gonzalez-Fierro et al., 2011). Hydralazine area under the curve plasma levels were 2.2-fold higher in slow than in rapid acetylators, which subsequently has been used as a rationale for prescribing hydralazine doses 2.2-fold lower in slow (83 mg) than in rapid (182 mg) acetylators. This dose adjustment yielded similar plasma levels of hydralazine in rapid and slow acetylators in several studies (Arce et al., 2006;

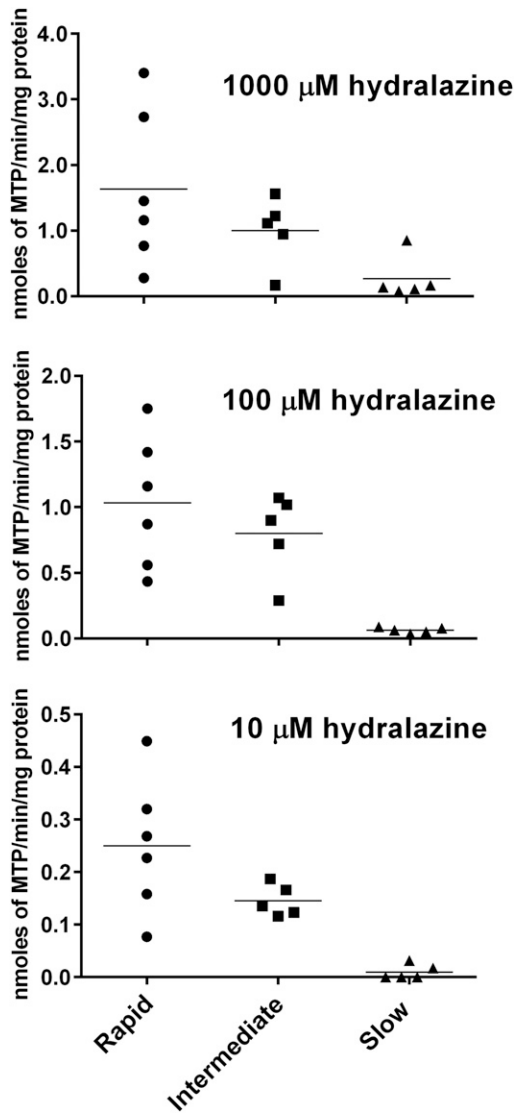


Fig. 3. Hydralazine NAT activities in vitro in cryopreserved human hepatocytes from rapid, intermediate and slow NAT2 acetylators. Scatter plots illustrate hydralazine NAT activities in vitro in cryopreserved human hepatocytes from rapid ($n = 6$), intermediate ($n = 5$), and slow ($n = 5$) NAT2 acetylators. Hydralazine NAT activities differed significantly with respect to NAT2 phenotype at each concentration tested (in μM hydralazine): 1000 ($P = 0.0319$); 100 ($P = 0.002$); and 10 ($P = 0.0029$).

Gonzalez-Fierro et al., 2011; Garcés-Eisele et al., 2014) with at least one exception in a study from the same group (Candelaria et al., 2007). Although none of these studies measured MTP levels, they appear to be the experimental basis for clinical trials using a hydralazine dosing strategy of 83 mg in slow acetylators and 183 mg in rapid acetylators (either alone or in combination with other drugs such as valproic acid) for the epigenetic treatment of cancer. A dosing strategy for intermediate acetylators is not stated.

In a recent study (Spinasse et al., 2014), DNA samples from 169 patients with resistant hypertension treated with hydralazine were identified as rapid (12.4%), intermediate (38.5%), and slow (35.5%) acetylators (13.6% indeterminate), as deduced from NAT2 genotype. In this group of patients treated with hydralazine, only slow acetylators had significant blood pressure reductions, although they also had a higher incidence of adverse effects; neither hydralazine nor MTP plasma levels were reported.

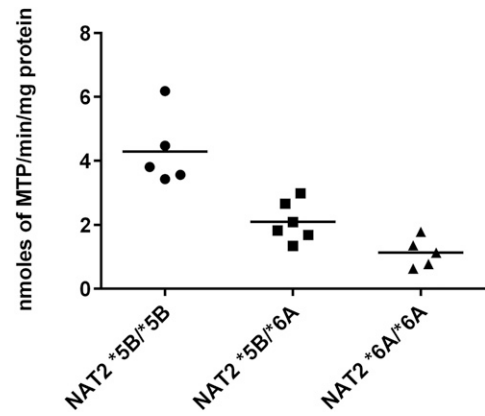


Fig. 4. Hydralazine NAT activities in vitro in cryopreserved human hepatocytes among slow NAT2 acetylator genotypes. Scatter plots illustrate hydralazine NAT activities in vitro in cryopreserved human hepatocytes with NAT2*5B/*5B ($n = 5$), NAT2*5B/*6A ($n = 6$), and NAT2*6A/*6A ($n = 5$) genotypes. Hydralazine NAT activities differed significantly with respect to slow acetylator NAT2 genotype ($P < 0.001$).

After recombinant expression in yeast, we confirmed that NAT2 is the primary NAT responsible for acetylation of hydralazine at therapeutic concentrations based on the lower apparent K_m value, signifying increased affinity, and the higher apparent V_{max} leading to a 50-fold higher hydralazine *N*-acetylation clearance by NAT2 than NAT1.

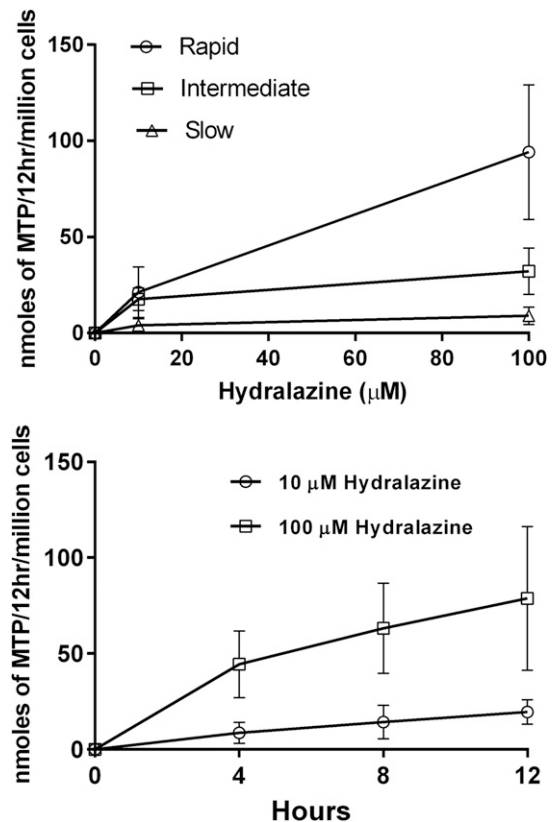


Fig. 5. Concentration- and time-dependent *N*-acetylation of hydralazine in cryopreserved human hepatocytes in situ. Cryoplateable human hepatocytes were plated on collagen-coated 12-well plates and allowed to attach. After 48 hours, plating media were removed, and cells were washed then grown with PBS + dextrose containing (0–100 μM) hydralazine for 12 hours. (Top) Each data point illustrates the mean \pm S.D. in cryopreserved human hepatocytes from five individual rapid, intermediate, or slow acetylators. (Bottom) Each data point illustrates the mean \pm S.D. in cryopreserved human hepatocytes from five individual rapid acetylators.

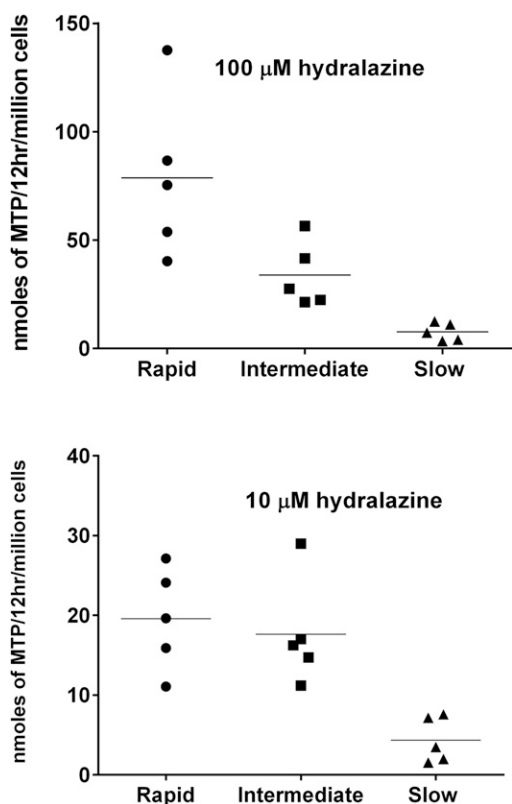


Fig. 6. *N*-Acetylation of hydralazine in situ in cryopreserved human hepatocytes from rapid, intermediate, and slow acetylators. Cryoplateable human hepatocytes were plated on collagen-coated 12-well plates and allowed to attach. After 48 hours, plating media were removed, and cells were washed then grown with PBS + dextrose containing 10 or 100 μM hydralazine for 12 hours. Scatter plots illustrate hydralazine *N*-acetylation rates in rapid ($n = 5$), intermediate ($n = 5$), and slow ($n = 5$) acetylator cryopreserved human hepatocytes after incubation with 100 μM (top) and 10 μM (bottom) hydralazine. Hydralazine *N*-acetylation rates differed significantly among the rapid, intermediate, and slow acetylator cryopreserved human hepatocytes at 10 μM ($P = 0.002$) and 100 μM ($P = 0.0015$) hydralazine.

We investigated the *N*-acetylation of hydralazine in cryopreserved human hepatocytes from rapid, intermediate, and slow acetylators. Key findings in our study support a three-tier “trimodal” acetylating variation, with phenotypic differences observed among rapid, intermediate, and slow NAT2 genotypes. Although we observed overlap in hydralazine *N*-acetylation rates among the NAT2 rapid, intermediate, and slow acetylator genotypes, nevertheless *N*-acetylation of hydralazine was NAT2 genotype dependent with the relative magnitude of differences between acetylator phenotypes dependent upon hydralazine concentration (and presumably on hydralazine dosing regimen). The Michaelis-Menten kinetic analysis of human NAT1 and NAT2 after recombinant expression in yeast suggests that NAT1 may contribute to the *N*-acetylation of hydralazine, particularly at higher hydralazine concentrations. Thus, the role of NAT2 genotype on hydralazine efficacy and toxicity may be greater after lower dosing regimens. Furthermore, we observed small but highly significant ($P < 0.001$) differences among slow acetylator genotypes supporting the concept of an acetylating index, as previously described for hydralazine (Shepherd et al., 1981) and more recently reported (Doll and Hein, 2017) in cryopreserved human hepatocytes for the same probe drug (sulfamethazine).

Hydralazine *N*-acetylation was both time and concentration dependent in situ in cryopreserved human hepatocytes. Cryopreserved hepatocytes with rapid, intermediate, and slow acetylator genotypes produced the most, moderate, and least amount of MTP, respectively.

Thus, both the in vitro and in situ results in cryopreserved human hepatocytes support the trimodal model of hydralazine acetylation. An important finding during the in situ studies was the instability of hydralazine in most growth media. We conducted HPLC analysis of hydralazine in different types of media and found hydralazine to be unstable in all media tested and only stable in PBS. Therefore, after plating hepatocytes in the normal growth media for 48 hours, we cultured the hepatocytes in PBS + dextrose when incubating them with hydralazine to ensure that the cells were receiving the appropriate concentration of hydralazine.

Our results clearly document NAT2 genotype-dependent *N*-acetylation of hydralazine in human hepatocytes, suggesting that hydralazine efficacy and safety could be improved by NAT2 genotype-dependent dosing strategies. More specific dosing strategies, particularly in epigenetic clinical trials, could facilitate maximal therapeutic benefit from hydralazine.

Acknowledgments

We thank Timothy Moeller and BioreclamationIVT for their valuable contributions. We also thank Samantha Carlisle, Raul Salazar-González, and Marcus Stepp for their review of and suggestions to improve the manuscript.

Authorship Contributions

Participated in research design: Allen, Doll, and Hein.

Conducted experiments: Allen and Doll.

Performed data analysis: Allen, Doll, and Hein.

Wrote or contributed to the writing of the manuscript: Allen, Doll, and Hein.

References

- Arce C, Pérez-Plascencia C, González-Fierro A, de la Cruz-Hernández E, Revilla-Vázquez A, Chávez-Blanco A, Trejo-Becerril C, Pérez-Cárdenas E, Taja-Chayeb L, Bargallo E, et al. (2006) A proof-of-principle study of epigenetic therapy added to neoadjuvant doxorubicin cyclophosphamide for locally advanced breast cancer. *PLoS One* 1:e98.
- Candelaria M, Gallardo-Rincón D, Arce C, Cetina L, Aguilar-Ponce JL, Arrieta O, González-Fierro A, Chávez-Blanco A, de la Cruz-Hernández E, Camargo MF, et al. (2007) A phase II study of epigenetic therapy with hydralazine and magnesium valproate to overcome chemotherapy resistance in refractory solid tumors. *Ann Oncol* 18:1529–1538.
- Castillo-Aguilera O, Depreux P, Halby L, Arimondo PB, and Goossens L (2017) DNA methylation targeting: the DNMT/HMT crosstalk challenge. *Biomolecules* 7:3.
- Chuang JC, Yoo CB, Kwan JM, Li TW, Liang G, Yang AS, and Jones PA (2005) Comparison of biological effects of non-nucleoside DNA methylation inhibitors versus 5-aza-2'-deoxycytidine. *Mol Cancer Ther* 4:1515–1520.
- Cohn JN, McInnes GT, and Shepherd AM (2011) Direct-acting vasodilators. *J Clin Hypertens (Greenwich)* 13:690–692.
- Coronel J, Cetina L, Pacheco I, Trejo-Becerril C, González-Fierro A, de la Cruz-Hernandez E, Perez-Cardenas E, Taja-Chayeb L, Arias-Bofill D, Candelaria M, et al. (2011) A double-blind, placebo-controlled, randomized phase III trial of chemotherapy plus epigenetic therapy with hydralazine valproate for advanced cervical cancer. Preliminary results. *Med Oncol* 28 (Suppl 1): S540–S546.
- Doll MA and Hein DW (2001) Comprehensive human NAT2 genotype method using single nucleotide polymorphism-specific polymerase chain reaction primers and fluorogenic probes. *Anal Biochem* 288:106–108.
- Doll MA and Hein DW (2017) Genetic heterogeneity among slow acetylator *N*-acetyltransferase 2 phenotypes in cryopreserved human hepatocytes. *Arch Toxicol* 91:2655–2661.
- Doll MA, Salazar-González RA, Bodduluri S, and Hein DW (2017) Arylamine *N*-acetyltransferase 2 genotype-dependent *N*-acetylation of isoniazid in cryopreserved human hepatocytes. *Acta Pharm Sin B* 7:517–522.
- Dueñas-González A, Coronel J, Cetina L, González-Fierro A, Chavez-Blanco A, and Taja-Chayeb L (2014) Hydralazine-valproate: a repositioned drug combination for the epigenetic therapy of cancer. *Expert Opin Drug Metab Toxicol* 10:1433–1444.
- Garcés-Eisele SJ, Cedillo-Carvallo B, Reyes-Núñez V, Estrada-Marín L, Vázquez-Pérez R, Juárez-Calderón M, Guzmán-García MO, Dueñas-González A, and Ruiz-Argüelles A (2014) Genetic selection of volunteers and concomitant dose adjustment leads to comparable hydralazine/valproate exposure. *J Clin Pharm Ther* 39:368–375.
- Gonzalez-Fierro A, Vasquez-Bahena D, Taja-Chayeb L, Vidal S, Trejo-Becerril C, Pérez-Cardenas E, de la Cruz-Hernández E, Chávez-Blanco A, Gutiérrez O, Rodríguez D, et al. (2011) Pharmacokinetics of hydralazine, an antihypertensive and DNA-demethylating agent, using controlled-release formulations designed for use in dosing schedules based on the acetylator phenotype. *Int J Clin Pharmacol Ther* 49:519–524.
- Graça I, Sousa EJ, Costa-Pinheiro P, Vieira FQ, Torres-Ferreira J, Martins MG, Henrique R, and Jerónimo C (2014) Anti-neoplastic properties of hydralazine in prostate cancer. *Oncotarget* 5:5950–5964.
- Hein DW (2009) *N*-acetyltransferase SNPs: emerging concepts serve as a paradigm for understanding complexities of personalized medicine. *Expert Opin Drug Metab Toxicol* 5:353–366.
- Hein DW and Doll MA (2017) Role of the *N*-acetylation polymorphism in solithromycin metabolism. *Pharmacogenomics* 18:765–772.

- Magee LA, Cham C, Wateman EJ, Ohlsson A, and von Dadelzen P (2003) Hydralazine for treatment of severe hypertension in pregnancy: meta-analysis. *BMJ* **327**:955–960.
- McDonagh EM, Boukouvala S, Aklillu E, Hein DW, Altman RB, and Klein TE (2014) PharmGKB summary: very important pharmacogene information for N-acetyltransferase 2. *Pharmacogenet Genomics* **24**:409–425.
- Segura-Pacheco B, Perez-Cardenas E, Taja-Chayeb L, Chavez-Blanco A, Revilla-Vazquez A, Benitez-Bribiesca L, and Duenas-González A (2006) Global DNA hypermethylation-associated cancer chemotherapy resistance and its reversion with the demethylating agent hydralazine. *J Transl Med* **4**:32.
- Shepherd AM, McNay JL, Ludden TM, Lin MS, and Musgrave GE (1981) Plasma concentration and acetylator phenotype determine response to oral hydralazine. *Hypertension* **3**:580–585.
- Singh N, Dueñas-González A, Lyko F, and Medina-Franco JL (2009) Molecular modeling and molecular dynamics studies of hydralazine with human DNA methyltransferase 1. *ChemMedChem* **4**:792–799.
- Singh V, Sharma P, and Capalash N (2013) DNA methyltransferase-1 inhibitors as epigenetic therapy for cancer. *Curr Cancer Drug Targets* **13**:379–399.
- Spinasse LB, Santos AR, Suffys PN, Muxfeldt ES, and Salles GF (2014) Different phenotypes of the NAT2 gene influences hydralazine antihypertensive response in patients with resistant hypertension. *Pharmacogenomics* **15**:169–178.
- Tampe B, Tampe D, Zeisberg EM, Müller GA, Bechtel-Walz W, Koziolk M, Kalluri R, and Zeisberg M (2015) Induction of Tet3-dependent epigenetic remodeling by low-dose hydralazine attenuates progression of chronic kidney disease. *EBioMedicine* **2**:19–36.
- Weber WW and Hein DW (1985) N-acetylation pharmacogenetics. *Pharmacol Rev* **37**:25–79.

Address correspondence to: David W. Hein, Kosair Charities CTR-Room 303, 505 South Hancock St., Louisville, KY 40202. E-mail: d.hein@louisville.edu
